

# Magnetic Depth Profiling Co/Cu Multilayers to Investigate Magnetoresistance

J. Unguris,<sup>a</sup> D. Tulchinsky, M. H. Kelley, J. A. Borchers, J. A. Dura, , and C. F. Majkrzak

*National Institute of Standards and Technology  
Gaithersburg, Maryland 20899-8412*

S. Y. Hsu, R. Loloee, W. P. Pratt Jr. and J. Bass

*Department of Physics and Astronomy, Center for Fundamental Materials Research, and  
Center for Sensor Materials, Michigan State University  
East Lansing, Michigan, 48824*

The magnetic microstructure responsible for the metastable high resistance state of weakly coupled, as-prepared [Co(6nm)/Cu(6nm)]<sub>20</sub> multilayers was analyzed using polarized neutron reflectivity (PNR) and scanning electron microscopy with polarization analysis (SEMPA). This paper focuses and expands on the SEMPA measurements. In multilayer structures such as these, SEMPA can be combined with ion milling to directly image the layer-by-layer magnetization and quantitatively depth profile the interlayer magnetic domain correlations. We found that in the as-prepared Co/Cu multilayer the domains are about one micrometer in size and the magnetizations in adjacent layers are almost completely oppositely aligned. The relative magnetoresistance derived from this measured degree of anticorrelation is in agreement with the measured magnetoresistance.

---

<sup>a</sup> Electronic mail: john.unguris@nist.gov

## I. Introduction

Knowledge of the layer-by-layer magnetic microstructure of magnetic multilayers that exhibit giant magnetoresistance (GMR) is a critical part of understanding how these systems work. In particular, the spin dependent transport depends on the relative alignment of the magnetization between adjacent layers and how this alignment changes with applied magnetic field.<sup>1,2</sup> Imaging this buried magnetic structure is difficult. Imaging tools with deep probing depths may be used if the various layers are distinguishable. For example, layers that have different chemical compositions or tracer layers may be separated. In many relevant systems, however, such as the Co/Cu structure described in this paper, the magnetic layers are identical and it is difficult to separate the information from the various layers. We have successfully depth profiled the layer-by-layer magnetic microstructure of such multilayers by combining a surface sensitive magnetic imaging technique, scanning electron microscopy with polarization analysis (SEMPA), with ion milling.

Weakly coupled CoCu layers are of interest for potential GMR sensor applications. These multilayers have the interesting property that the resistance of the as-prepared state, i.e. the asgrown multilayer before applying a magnetic field, is often larger than the resistance at the coercive field,<sup>3</sup> and this initial resistance cannot be restored after cycling the applied magnetic field or by demagnetization.<sup>4,5</sup> In a previous report<sup>6</sup> the magnetic microstructure responsible for this initial magnetoresistance was resolved by using a combination of polarized neutron reflectivity (PNR),<sup>7,8,9,10</sup> which probes the magnetic order of the entire sample, and (SEMPA),<sup>11</sup> which provides a direct image of the magnetic structure one layer at a time. Both the SEMPA and PNR measurements showed that the large magnetoresistance of the as-prepared state is due to strong antiparallel correlations among the Co domain magnetizations across the Cu layers. In the coercive state, PNR measurements found that the domains in adjoining layers are uncorrelated.

In this paper we give an expanded description of the SEMPA measurements. In particular, we describe how SEMPA can be combined with ion milling to depth profile the magnetic structure of multilayers such as these. The SEMPA images provide

quantitative information about the magnetic correlations in adjacent layers that are in agreement with the measured GMR values of these multilayers.

## II. Experimental Results

The techniques used to make the  $[\text{Co}(6\text{nm})/\text{Cu}(6\text{nm})]_{20}$  multilayer that we studied by SEMPA are described elsewhere.<sup>12</sup> Bulk magnetization measurements revealed that the Co magnetization was in-plane, and the GMR values of the as-prepared and coercive states were 6.6% and 4.0%, respectively.<sup>6</sup> Ion milling, SEMPA imaging, and Auger compositional analysis were all done *in situ* using a small piece of the larger sample used for the MR and PNR measurements

Ion milling was carried out with a focused ion beam using 2 keV  $\text{Ar}^+$  ions. A scanning electron microscope (SEM) image of a flat bottomed, ion milled crater is shown in Fig. 1. In the SEM images the Cu layers appear brighter than the Co layers due to the larger secondary yield from Cu. A line scan across one edge of the crater measuring the Cu and Co Auger signals is also shown in Fig. 1. These line scans indicate that there is some mixing of the Co and Cu layers, however the layers are clearly chemically distinguishable for depths of at least 10 Co layers. This observed level of ion induced mixing is in rough agreement with an expected ion milling depth resolution of about 5 nm for this sample/ion combination.<sup>13</sup> Better depth resolution can be achieved by using lower ion energies, sample rotation, or molecular ions, such as  $\text{SF}_6$ .

The separation of the magnetic signal from adjacent Co layers is demonstrated in Fig. 2 which shows SEMPA images from a small ion milled crater in the as-prepared multilayer. In general, SEMPA measures the secondary electron intensity and two orthogonal polarizations, thereby simultaneously imaging the topography and two magnetization components. The topography and one magnetization component are shown in Fig. 2. The magnetization image shows that, for the most part, the magnetic structure from each Co layer is well separated from the other Co layers. Closer examination of the higher magnification SEMPA image in Fig. 2 reveals that a weak magnetic signal does appear in the Cu layers, especially for the deeper layers. This signal results from the ion induced mixing of the Co/Cu interfaces and from the finite probing depth ( $1/e$  about 1nm)

of the SEMPA measurement. This ability to see through to the layer below helps establish that no dramatic changes in the domain structure of the buried layers occur as we remove the outermost Co layers.

To image the layer-by-layer magnetic structure a large ( $2 \text{ mm}^2$ ) *flat bottomed* crater, such as the one shown in Fig. 1, was ion milled into the multilayer while monitoring the Co Auger signal from the center of the crater. The milling was terminated and SEMPA images were acquired from the center of the ion milled region each time the Co signal was maximized. SEMPA images from the first (outermost) Co layer acquired after removing the protective Cu capping layer are shown in Fig. 3. In this figure, the two SEMPA images of the orthogonal in-plane magnetization components have been combined to produce the color images of the magnetization direction. The magnetization directions are given by the color wheel in the inset of Fig. 3.

The domain structure of the as-prepared Co layer has several general features. First, the nominal domain size is about  $1 \text{ }\mu\text{m}$ . However, the domains shapes are very irregular with feature sizes ranging from a few tenths of a  $\mu\text{m}$  to tens of  $\mu\text{ms}$ . Second, the domains are separated by Néel type domain walls that are about  $200 \text{ nm}$  wide and have random chiralities. Both the domains and domain walls are larger than the average grain size of the film, which from the SEMPA topography images appears to be about  $100 \text{ nm}$  or less. Finally, the magnetization appears to be uniaxial. A histogram of the magnetization directions shown in the inset in Fig. 3 clearly shows that the magnetization is distributed along a single axis as if there were a strong uniaxial anisotropy. This anisotropy was not observed in the PNR measurements. This can be reconciled if the anisotropy direction varies over the sample since it would then be averaged out in the neutron measurements. However, SEMPA images sampling an area that is about one quarter of that probed in the PNR measurements only show a single anisotropy direction.

Layer-by-layer domain correlations were analyzed by using SEMPA images of consecutive layers. Figure 4 shows the magnetic structure of the first (outermost) Co layer and the second Co layer. Qualitatively, one can see from these images that the domains in these layers are anticorrelated. This anticorrelation even extends to details as small as the domain walls. The magnetization directions within domain walls in the adjacent layers are predominately in opposite directions, so that the domain wall chirality

remains the same in all the layers. Arrows in the SEMPA images in Fig. 4 point to examples of this domain wall anticorrelation.

To quantify the magnetic correlations, the magnetic images are first brought into exact registry by aligning the simultaneously acquired topographic images. The degree of magnetic correlation can then be determined by simply subtracting the two images of magnetization direction and plotting a histogram of this difference angle as shown in Fig. 4 (a). Since difference angles of  $-360^\circ$ ,  $0^\circ$ , and  $360^\circ$  ( $-180^\circ$  and  $180^\circ$ ) all correspond to ferromagnetic (antiferromagnetic) alignment, this histogram is further simplified by changing to a reduced difference angle,  $0^\circ \leq \Delta\phi \leq 180^\circ$ , such that  $\Delta\phi$  equals  $0^\circ$  ( $180^\circ$ ) for ferromagnetic (antiferromagnetic) alignment of the Co magnetization. Figure 4(b) shows the resulting, normalized distribution,  $P(\Delta\phi)$ , of the magnetic alignment. It is obvious from this distribution that the magnetization is strongly anticorrelated in these adjacent layers.

To determine if this measured correlation function can account for the measured magnetoresistance of the multilayer we use the following model. We assume that the resistance,  $R(\Delta\phi)$ , can be separated into a magnetization independent term,  $R_0$ , and a magnetic alignment dependent term,  $R_M \cos(\Delta\phi)$ , such that:

$$R(\Delta\phi) = R_0 - R_M \cos(\Delta\phi) \quad (1)$$

The total resistance,  $\bar{R}$ , is then determined by integrating over the measured distribution of magnetization directions. This leads to the following relationship between the normalized relative magnetoresistance and the correlation distribution,  $\int P(\Delta\phi) \cos(\Delta\phi)$ , measured by SEMPA:

$$\frac{\bar{R} - R_0}{R_M} = - \int P(\Delta\phi) \cos(\Delta\phi) \quad (2)$$

For perfect ferromagnetic (antiferromagnetic) alignment this normalized resistance is therefore -1.0 (1.0). The normalized relative magnetoresistance determined from the measured  $P(\Delta\phi)$  distribution in Fig. 4(b) is  $0.62 \pm 0.05$ .

To compare this result from the SEMPA measurement with the MR measurements, the MR measurements need to be converted to the same normalized magnetoresistance. The conventional MR, as shown in Fig. 5, is given by:

$$MR = \frac{R(H) - R(H_{sat})}{R(H_{sat})} \quad (3)$$

The field dependent resistance,  $R(H)$ , and the resistance at saturation,  $R(H_{sat})$ , can be expressed in terms of the preceding model,  $R(H) = \bar{R}$  and  $R(H_{sat}) = R_0 - R_M$ . There is therefore a linear relationship between MR and the normalized relative magnetoresistance, and the scale factors are determined by first assuming that at large applied magnetic fields the Co layers are completely ferromagnetically aligned, so that a MR of 0 corresponds to a normalized relative magnetoresistance of -1. Second, we assume that at the coercive field there is no net magnetic correlation between the Co layers, so that, for this sample, a MR of 0.04 is equivalent to a normalized relative magnetoresistance of 0. The latter assumption is supported by PNR measurements of the coercive state which show only uncorrelated domains at the coercive field.<sup>6</sup> For this sample the normalized magnetoresistance is therefore equal to  $(MR/0.04) - 1$ . The MR data from this Co/Cu sample are plotted in Fig. 5 using both the conventional MR scale and the normalized relative resistance scale. From this figure one can see that the normalized resistance of the as-prepared state is 0.65 which agrees well with the resistance derived from the correlation measurement.

Depth profiling of the domain correlations by this method is not limited to the top two layers. Figure 6 shows SEMPA images from the top 10 Cu layers of a similar Co/Cu sample, but in a slightly different magnetic state. An unusual feature of this sample is that the magnetization rotates by  $90^\circ$  between the 2<sup>nd</sup> and 4<sup>th</sup> layers. This rotation can be clearly seen in the angular distribution histograms from the different layers shown in Fig.

6(a). It is not clear how the multilayer reached this magnetic state; perhaps the sample was slightly magnetized during handling. Surprisingly, however, the domains retained most of their correlation. The layer dependence of the normalized relative magnetoresistance derived from measuring the correlations between adjacent layers, and derived by computing the correlations with respect to the 4<sup>th</sup> layer are shown in Fig. 6(b). Although some small differences appear in the deeper layers, the domain structure and correlations appear to be relatively stable with prolonged ion milling.

One disadvantage of using an electron beam based measuring technique such as SEMPA is that it is difficult to image the sample in the presence of an applied magnetic field. For this sample, we were therefore unable to image the domain structure at the coercive field. We were able, however, to examine the domain correlations at remanence after magnetizing and demagnetizing the sample in various ways. In the simplest case, the sample's domain structure was profiled after applying a 1 kOe field to saturate the sample. The normalized relative resistance from the correlation measured by SEMPA for the resulting remanent state is  $-0.64 \pm 0.05$  which agrees well with the measured MR of  $-0.65$  in Fig. 5. Various demagnetization techniques were also attempted. The result of one interesting case is shown in Fig. 7 where the Co/Cu multilayer was demagnetized by rotating the sample in a decaying oscillating magnetic field. This treatment introduces closely packed  $360^\circ$  domain walls which are metastable in these very thin films.<sup>14</sup> Although superficially similar to the as prepared state, this structure was only slightly anticorrelated with a normalized relative resistance of 0.11. None of our demagnetization techniques were able to restore the domain structure of the as-prepared state.

### III. Discussion

It is somewhat surprising that depth profiling of these multilayers works as well as it appears to. After all, the magnetization, unlike the chemical structure, is not static and one might expect that the domain structure would change as a result of the ion milling. This sample has several characteristics that may make depth profiling by ion milling possible. First, the layers are as thick or thicker than the roughly 5 nm deep roughening and compositional mixing caused by the ion milling. Second, there are many

layers, so that removing one does not significantly change the magnetic structure and coupling of the rest. Third, the interlayer magnetic coupling is weak. There is sufficient magnetostatic or antiferromagnetic coupling to anticorrelate the magnetic domain structure as the multilayer is grown, but it is not enough to alter the established domain structure as layers are removed. Finally, we speculate that defects in the films, such as the observed granular structure, play an important role in partially stabilizing the magnetic domain structure, both while ion milling and while growing the multilayer. In general this depth profiling method should be applicable to multilayers with similar characteristics.

#### **IV. Conclusion**

We have shown that SEMPA can be used along with ion milling to depth profile the magnetic structure of weakly coupled magnetic multilayers. This method provides a direct picture of the layer-by-layer magnetic microstructure and allows a quantitative measurement of the interlayer magnetic correlations. The magnetic structure of a  $[\text{Co}(6\text{nm})/\text{Cu}(6\text{nm})]_{20}$  multilayer was characterized using SEMPA depth profiling, which images the magnetization one layer at a time, along with the complementary technique of PNR which simultaneously probes all of the Co layers. The SEMPA and PNR measurements of the as-prepared state reveal domains that are nominally  $1\ \mu\text{m}$  in size with strong antiparallel ordering between adjacent Co layers. The large MR of the as-prepared state is therefore due to this metastable antiparallel ordering which cannot be restored after cycling the magnetic field.

We have also shown that the magnetic correlations measured by SEMPA can, with a few assumptions, be directly related to the measured magnetoresistance. The normalized relative magnetoresistance derived from the magnetic correlations in the as-prepared and remanent states is in good agreement with the measured MR. A simple model using a cosine dependent magnetoresistance appears to adequately describe magnetization alignment dependence of the MR even in multilayers with small, complicated domain structures such as these.

## **Acknowledgements**

The authors are thankful to M. D. Stiles, R. J. Celotta and D. T. Pierce for helpful discussions. This work was supported by the Office Of Naval Research, and NSF grants: NSF DMR 98-20135 and MRSEC DMR 98-09688.

## References

- <sup>1</sup> P.M. Levy, *Solid State Physics Vol. 47*, H. Ehrenreich and D. Turnbull Eds., (Academic, New York,), 367 (1994).
- <sup>2</sup> J. Bass and W. P. Pratt, Jr., *J. Magn. Magn. Mat.* **200**, (1999).
- <sup>3</sup> W.P. Pratt, Jr., S.-F. Lee, J.M. Slaughter, R. Loloee, P.A. Schroeder and J. Bass, *Phys. Rev. Lett.* **66**, 3060 (1991).
- <sup>4</sup> P.A. Schroeder, S.-F. Lee, P. Holody, R. Loloee, Q. Yang, W.P. Pratt, Jr. and J. Bass, *J. Appl. Phys.* **76**, 6610 (1994).
- <sup>5</sup> Ch. Rehm, F. Klose, D. Nagengast, B. Pietzak, H. Maletta and A. Weidinger, *Physica B* **221**, 377 (1996).
- <sup>6</sup> J. A. Borchers, J. A. Dura, J. Unguris, D. Tulchinsky, M. H. Kelley, C. F. Majkrzak, S. Y. Hsu, R. Loloee, W. P. Pratt Jr., and J. Bass, *Phys. Rev. Lett.* **82**, 2796 (1999).
- <sup>7</sup> C.F. Majkrzak, *Physica B* **221**, 342 (1996).
- <sup>8</sup> S.K. Sinha, E.B. Sirota, S. Garoff and H.B. Stanley, *Phys. Rev. B* **38**, 2297 (1988); V. Holy and T. Baumbach, *Phys. Rev. B* **49**, 10668 (1994).
- <sup>9</sup> J.A. Borchers, P.M. Gehring, R.W. Erwin, J.F. Ankner, C.F. Majkrzak, T.L. Hylton, K.R. Coffey, M.A. Parker and J.K. Howard, *Phys. Rev. B* **54**, 9870 (1996).
- <sup>10</sup> S.K. Sinha in *Neutron Scattering in Materials Science II*, ed. by D.A. Neumann, T.P. Russell and B.J. Wuensch, *Mat. Res. Soc. Symp. Proc.* (Materials Research Society, Pittsburgh, 1995), Vol. **376**, p. 175.
- <sup>11</sup> M.R. Scheinfein, J. Unguris, M.H. Kelley, D.T. Pierce and R.J. Celotta, *Rev. Sci. Instrum.* **61**, 2501 (1990).
- <sup>12</sup> J.M. Slaughter, W.P. Pratt, Jr. and P.A. Schroeder, *Rev. Sci. Instrum.* **60**, 127 (1989).
- <sup>13</sup> L. S. Dake, D. E. King, J. R. Pitts, and A. W. Czanderna, in *Beam Effects, Surface Topography, and Depth Profiling*, A. W. Czanderna, T. E. Madey, and C. J. Powell, Eds. (Plenum Press, New York), 97 (1998)
- <sup>14</sup> A. Hubert and R. Schäfer, *Magnetic Domains (Springer, Berlin)*, 457 (1998).

## Figures

Fig.1 SEM image of an ion milled, flat bottomed crater, along with Cu and Co Auger line scans from one edge of the crater.

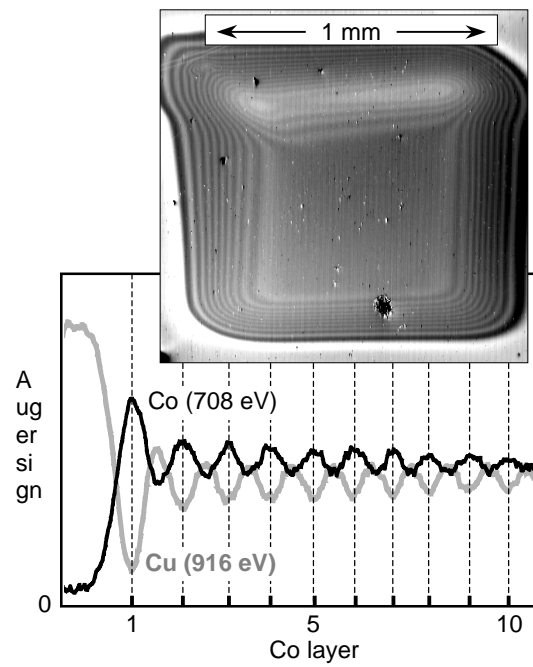


Fig. 1

Fig. 2 SEMPA images of the topography (intensity) and horizontal magnetization (polarization) component near a small ion milled crater. Light (dark) intensity bands correspond to Cu (Co) layers. The bottom image is a magnified view of the magnetization.

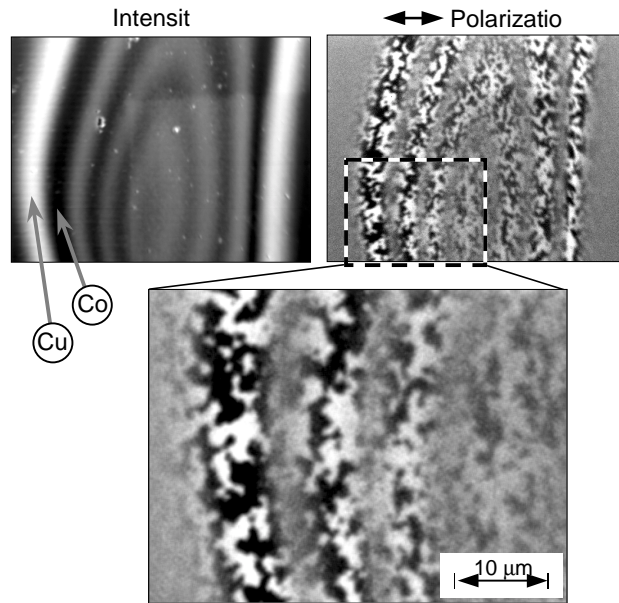


Fig. 2

Fig. 3 SEMPA images of topography and magnetization direction (color) of the outermost Co layer. The colorwheel shows the relationship between color and direction. A histogram of the magnetization direction from this image is shown in inset.

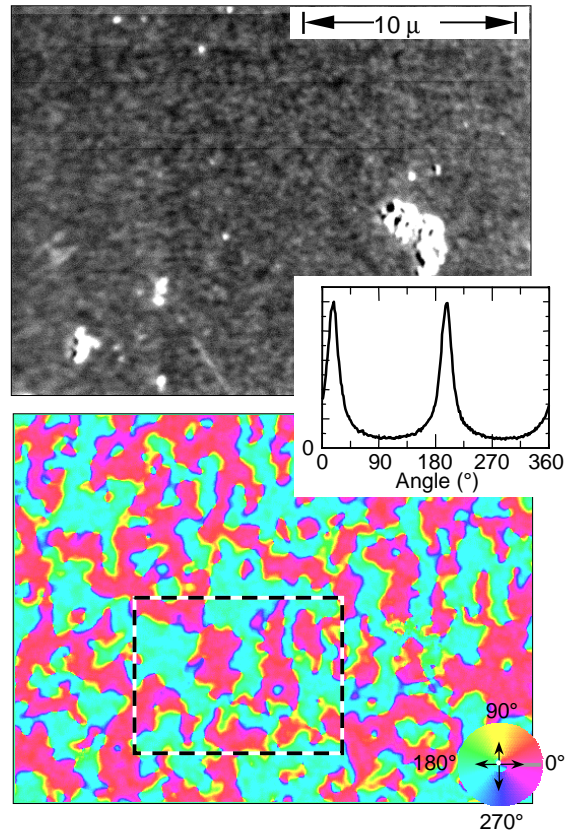


Fig. 3

Fig. 4 SEMPA images of 1<sup>st</sup> and 2<sup>nd</sup> Co layers from boxed area in Fig. 3. Histogram of difference in magnetization direction between these layers is shown in (a). The normalized angular distribution using the reduced angular scale is shown in (b).

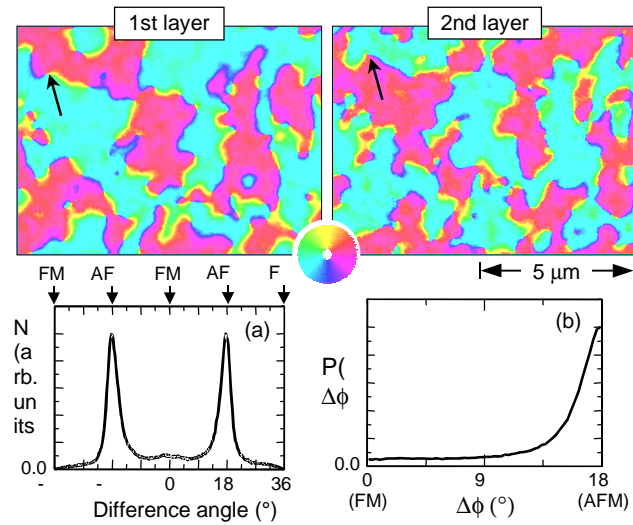


Fig. 4

Fig. 5 Measured MR for this sample. The normalized relative MR assuming the coercive state is uncorrelated is plotted along the right hand axis. The numbered circles point to normalized relative resistances derived from correlations measured by SEMPA for the as-prepared state (1), the remanent states following oscillating field demagnetization (2), and after saturation (3).

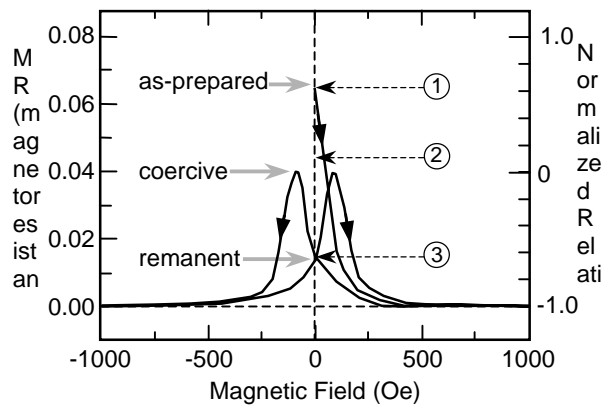


Fig. 5

Fig. 6 Depth profile through 10 Co layers. Histograms of the magnetization distributions are shown in (a) with the curves color-coded to the layer numbers in the SEMPA images. The normalized relative MR derived from correlations between adjacent layers (solid line) and relative to layer 4 (dotted line) is plotted in (b).

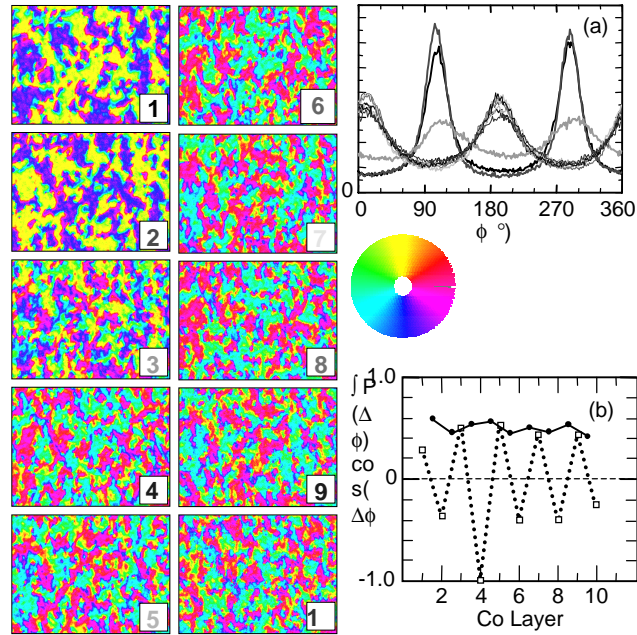


Fig. 6

Fig. 7 SEMPA images of 1<sup>st</sup> (outermost) and 2<sup>nd</sup> Co layers after demagnetizing sample in rotating field.

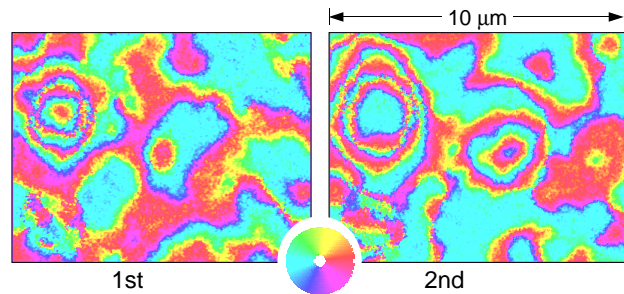


Fig. 7